Supplementary Figure 1

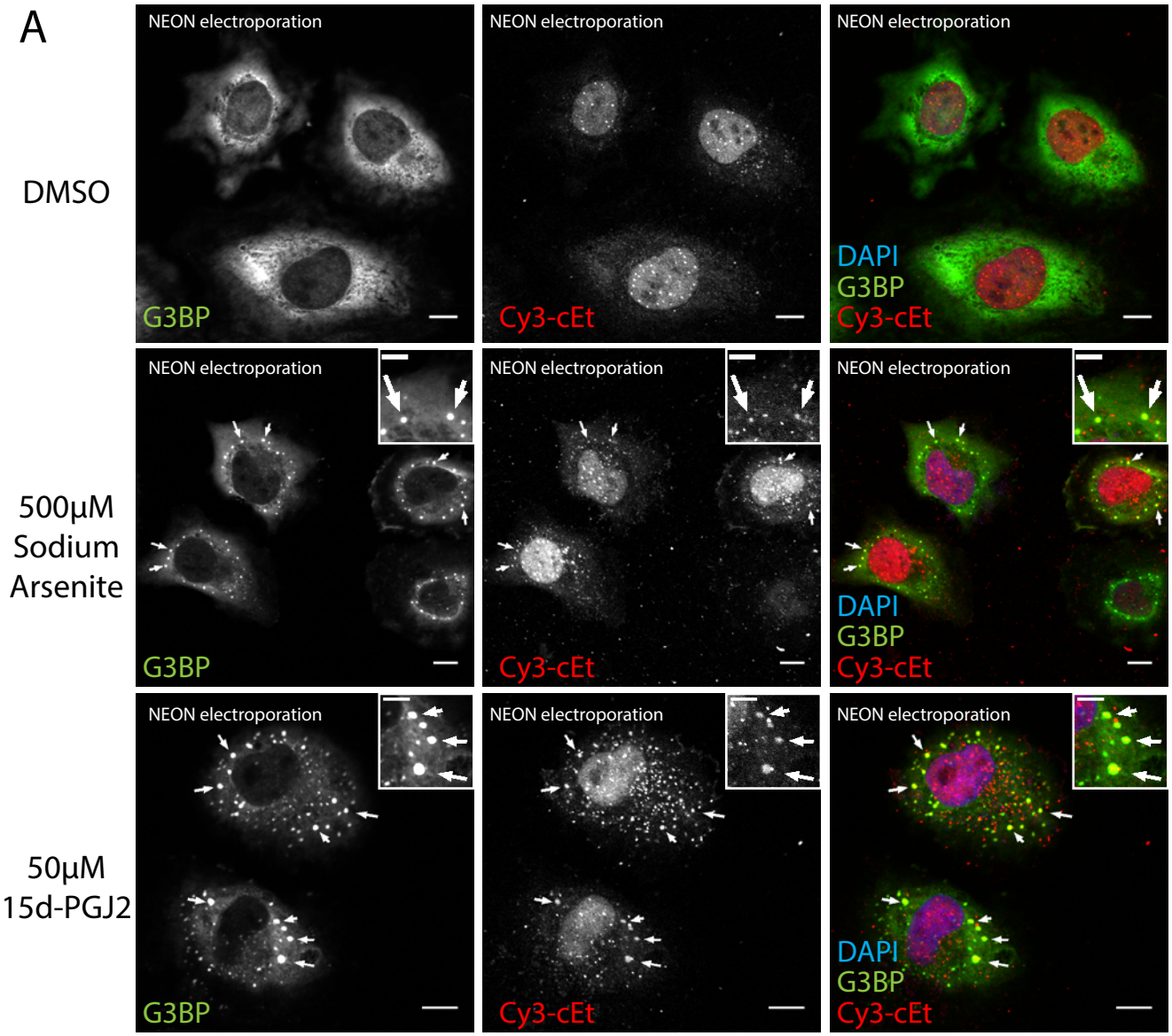

Supplementary Figure 2

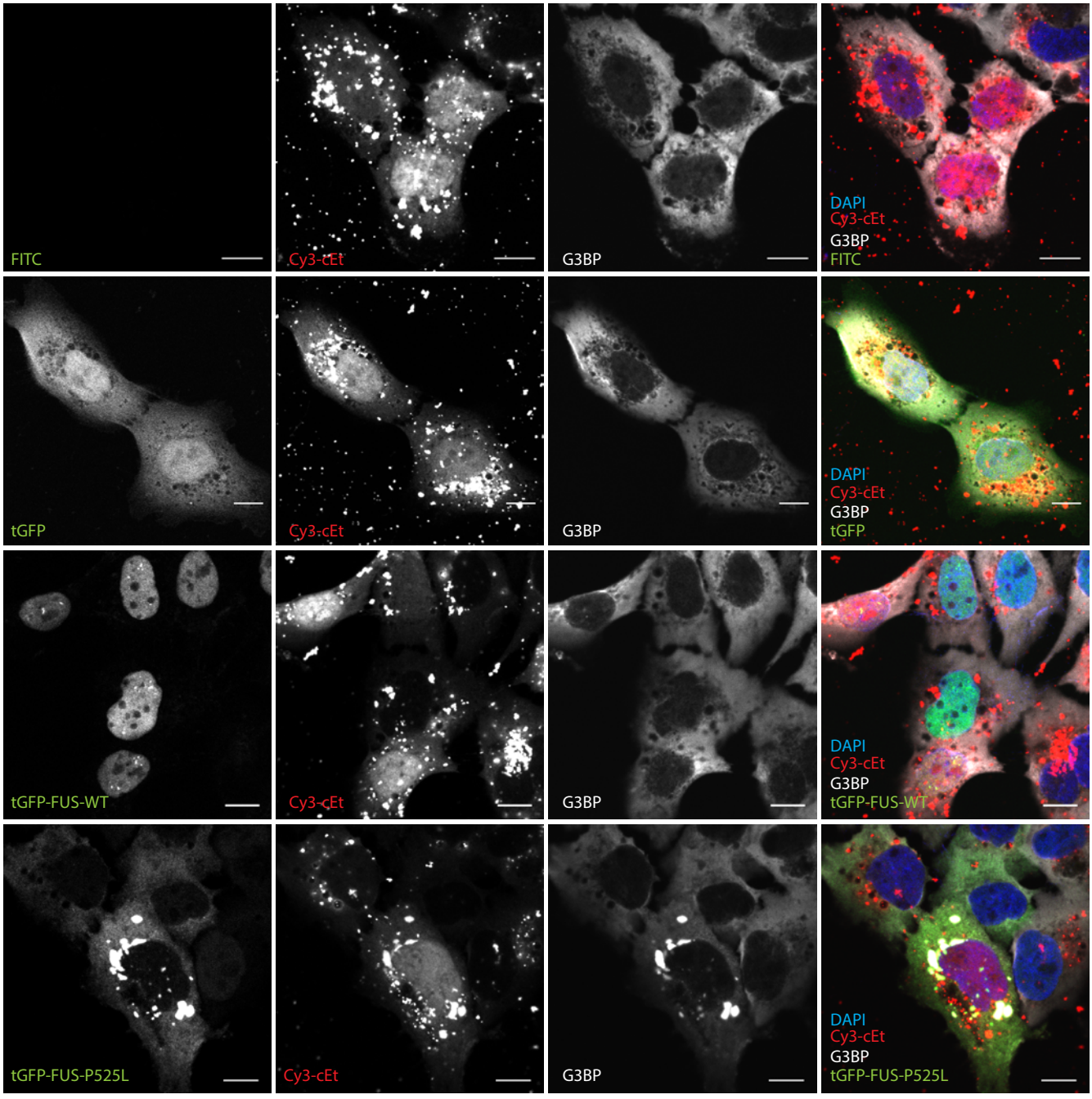

Supplementary Figure 3

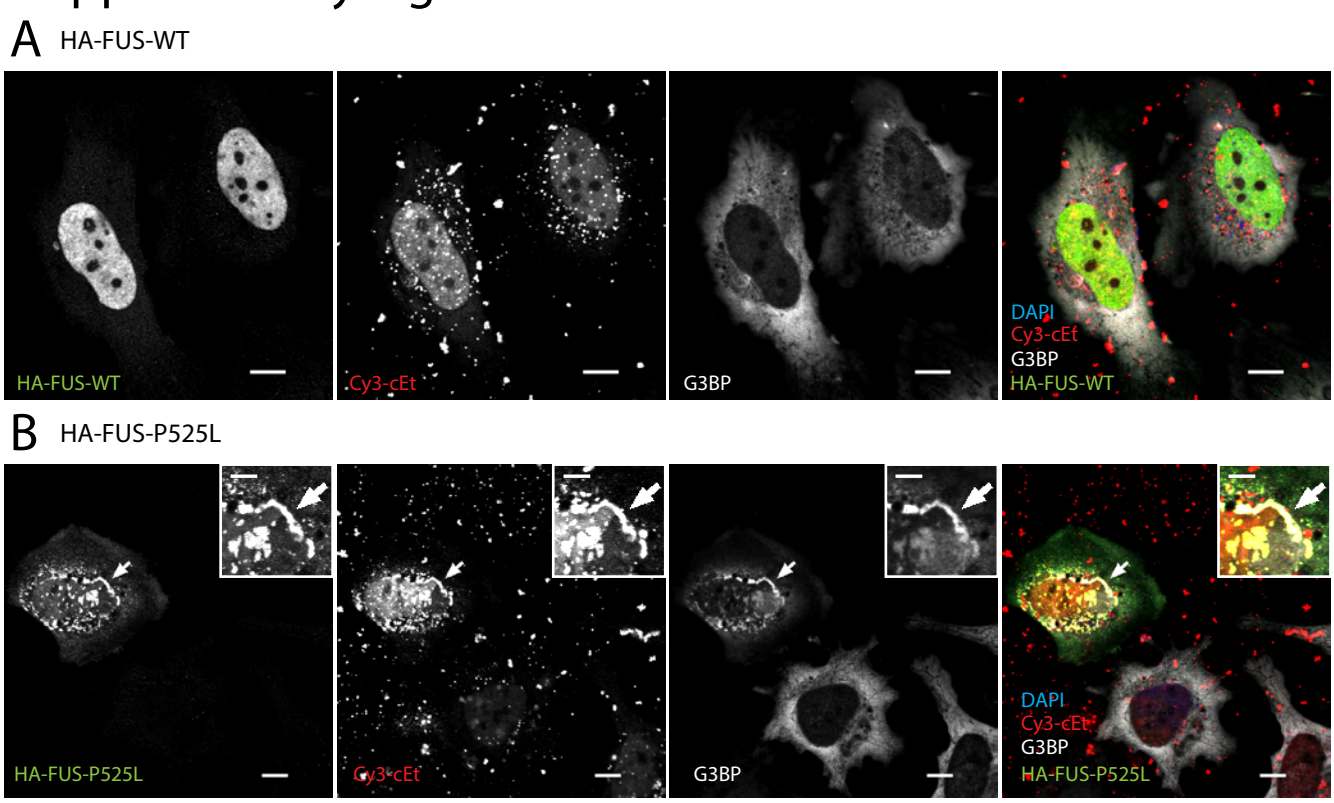

Supplementary Figure 4

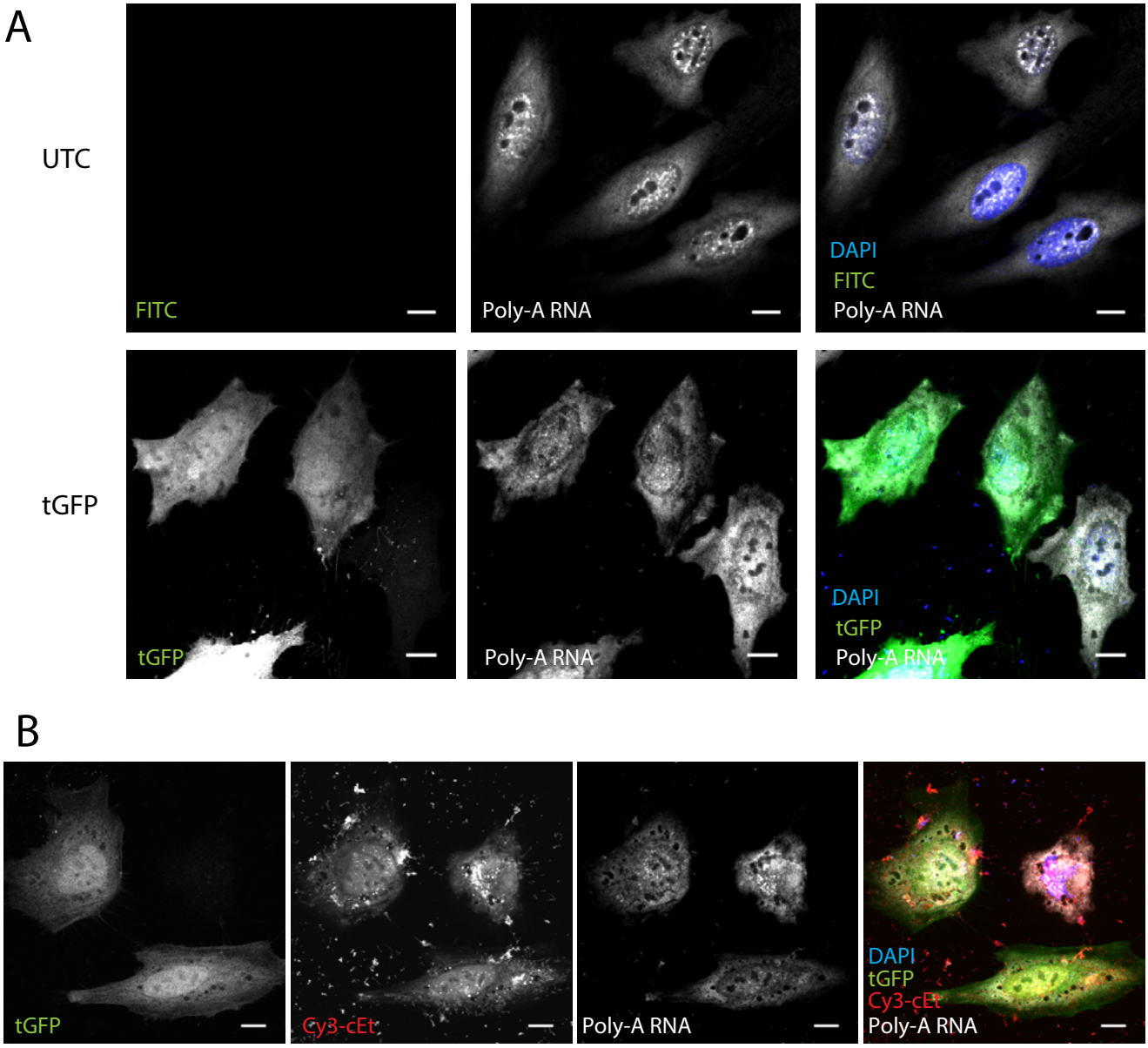

Supplementary Figure 5

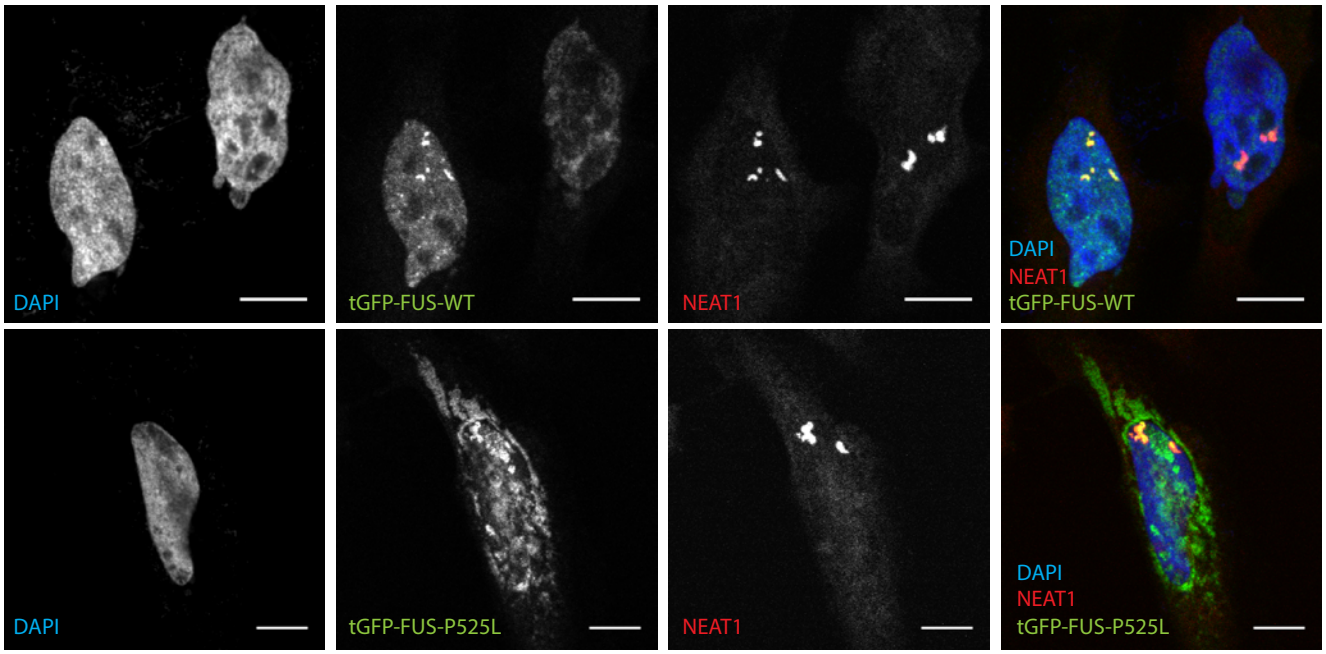

Supplementary Figure 6

A

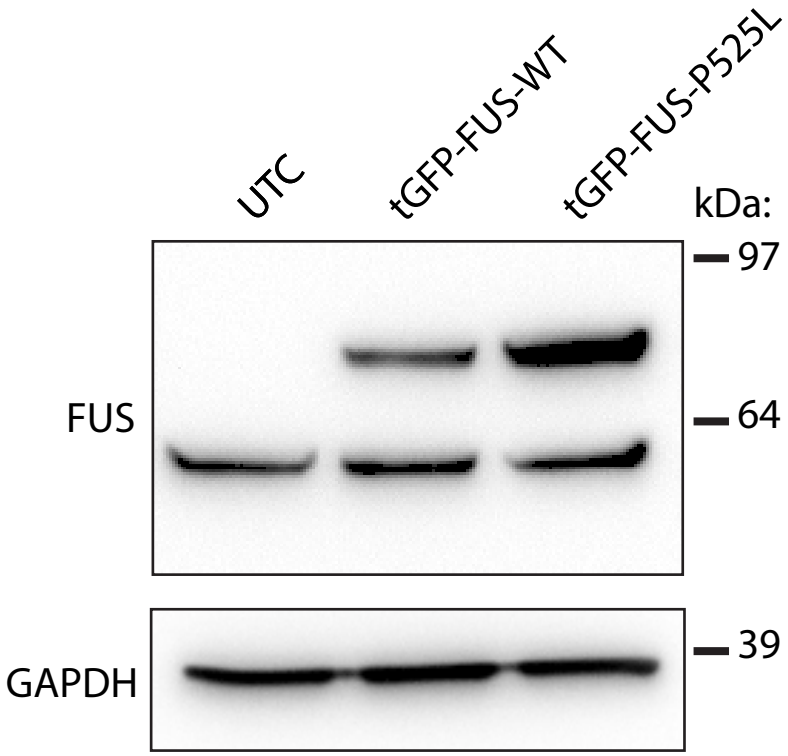

B

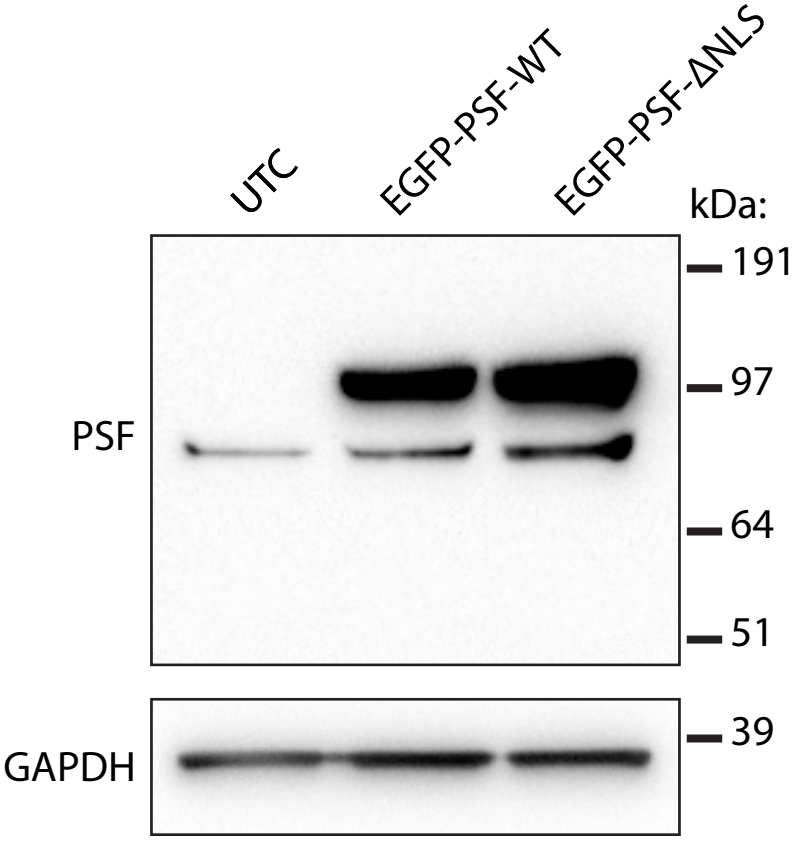

Supplementary Figure 7

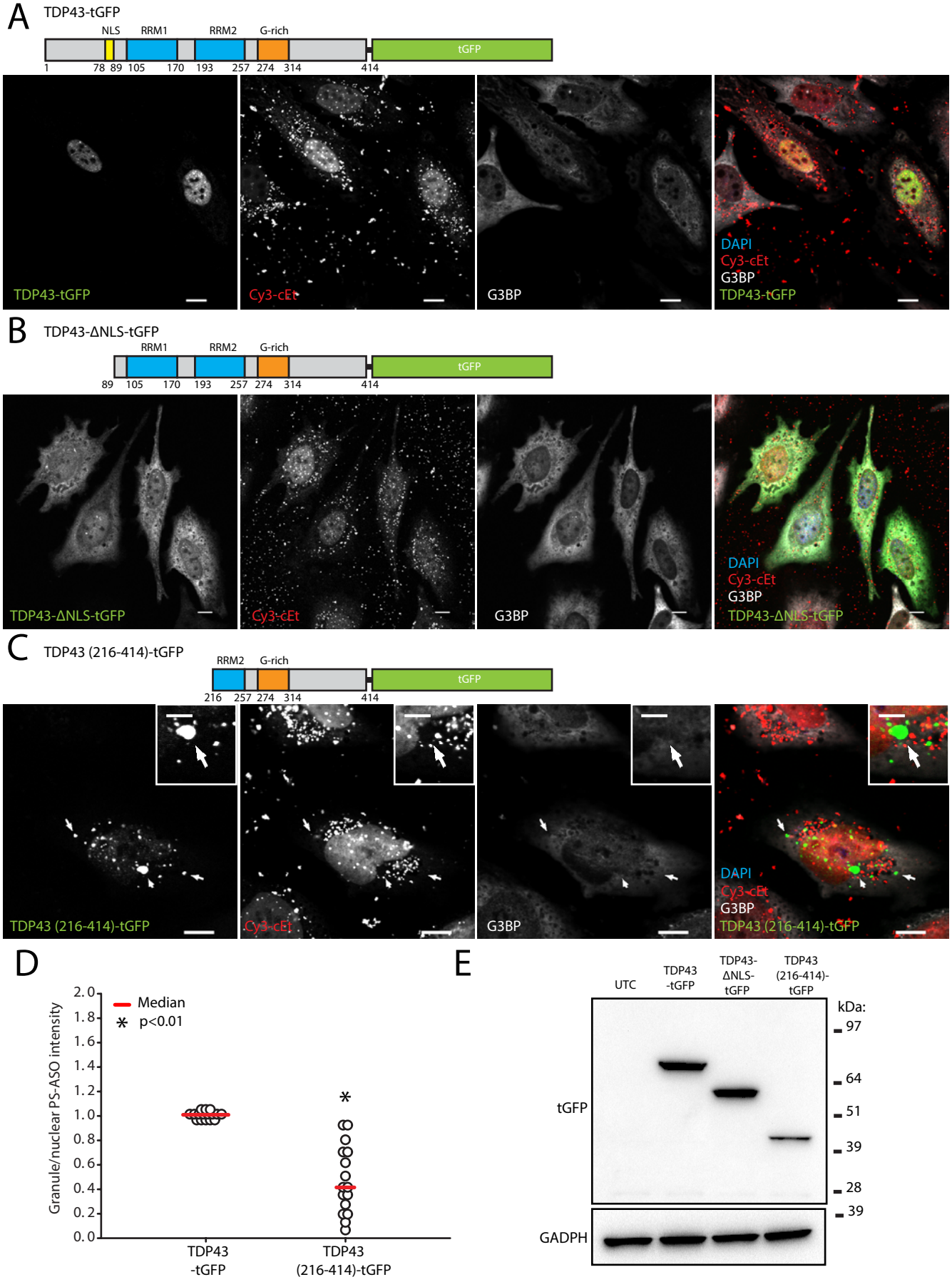

Supplementary Figure 8

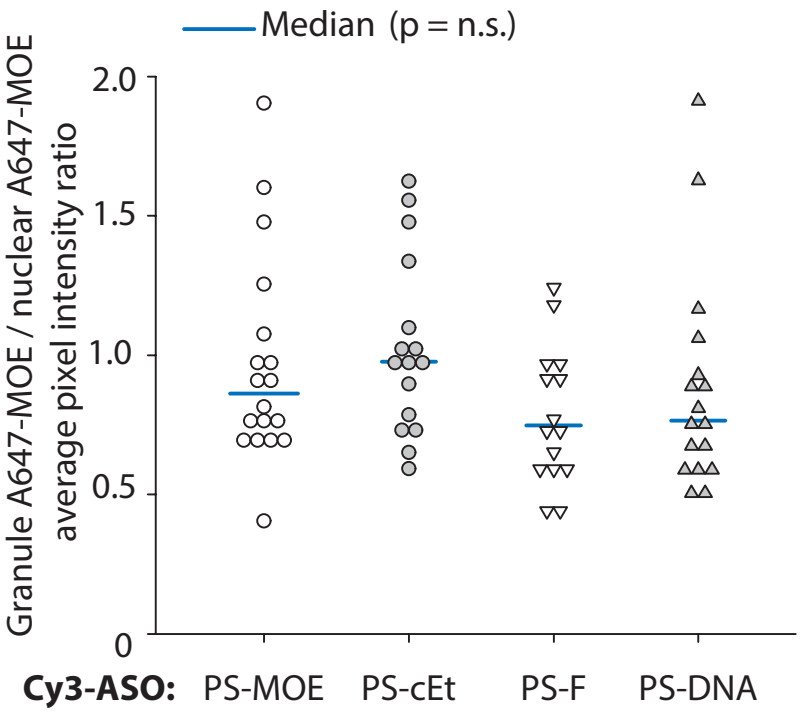

Supplementary Figure 9

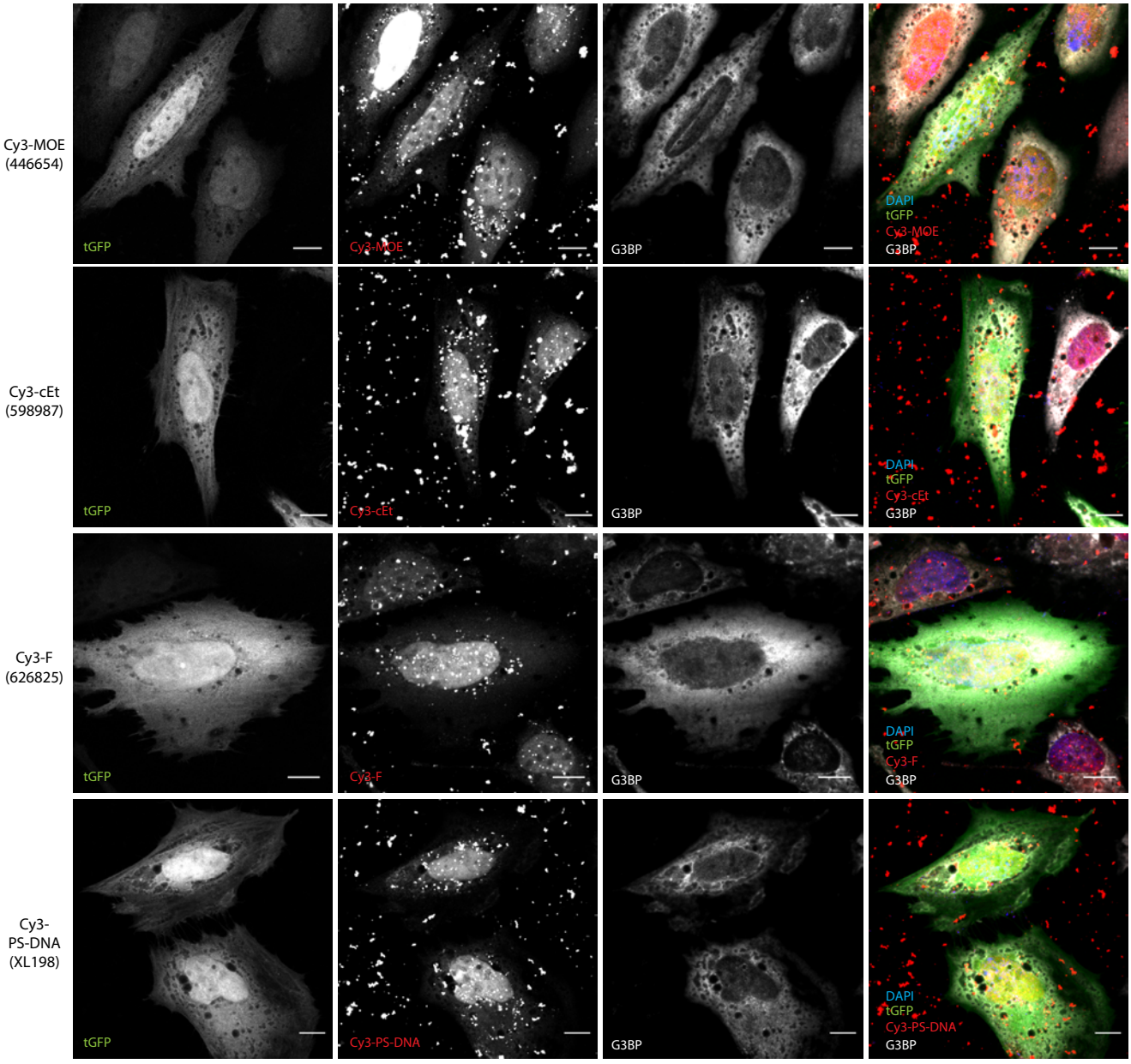

Supplementary Figure 10

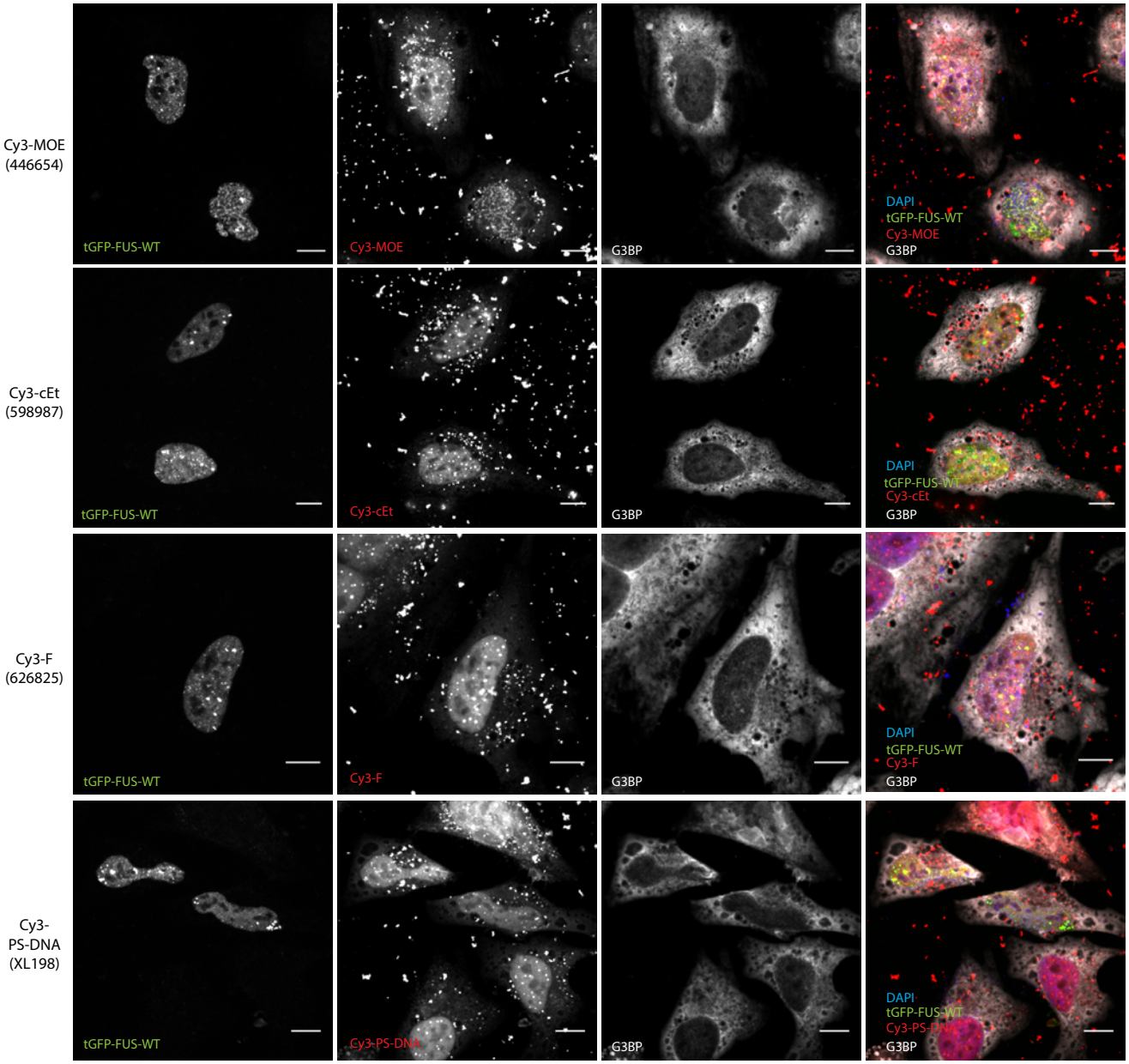

Supplementary Figure 11

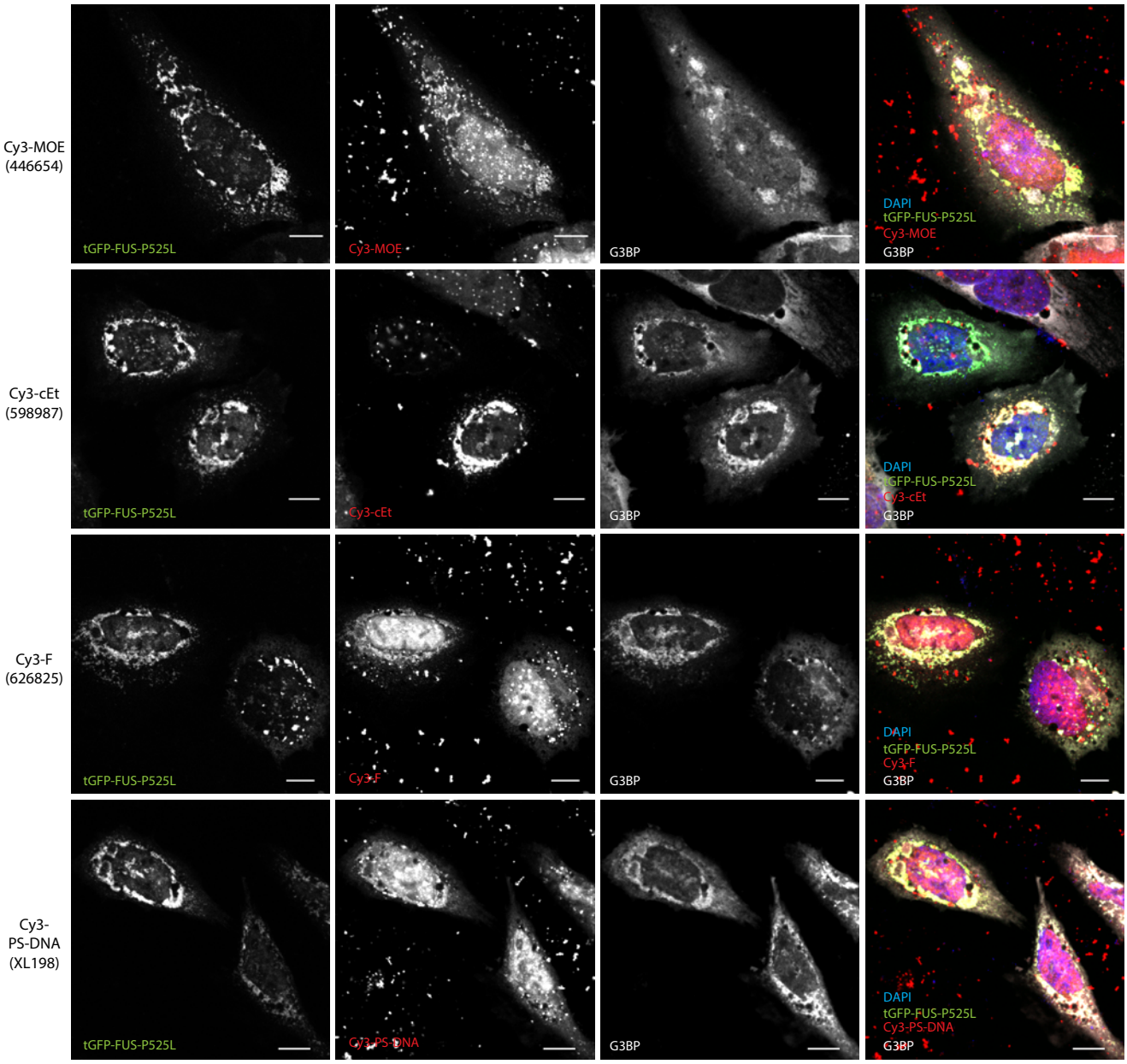

Supplementary Figure 12

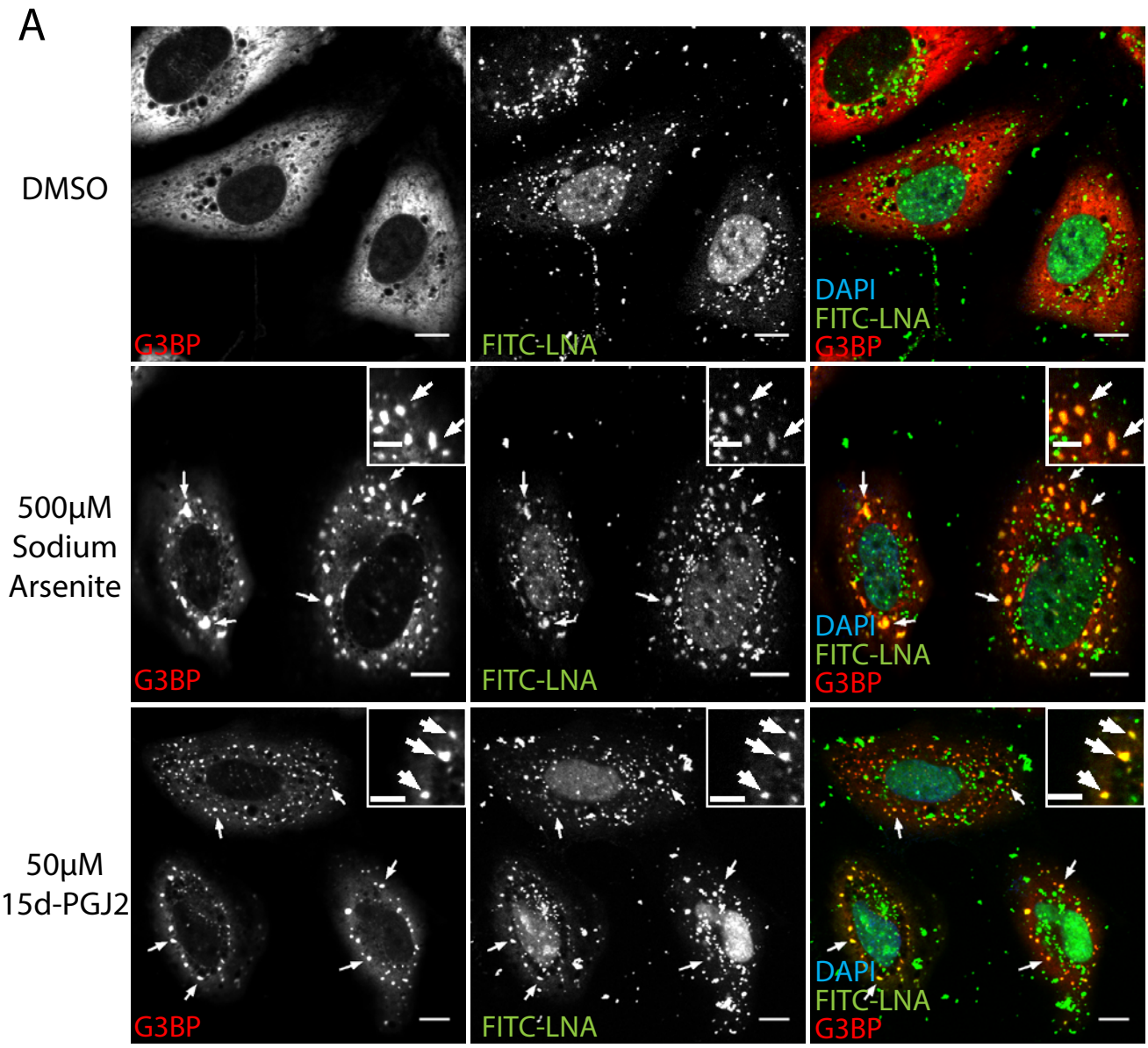

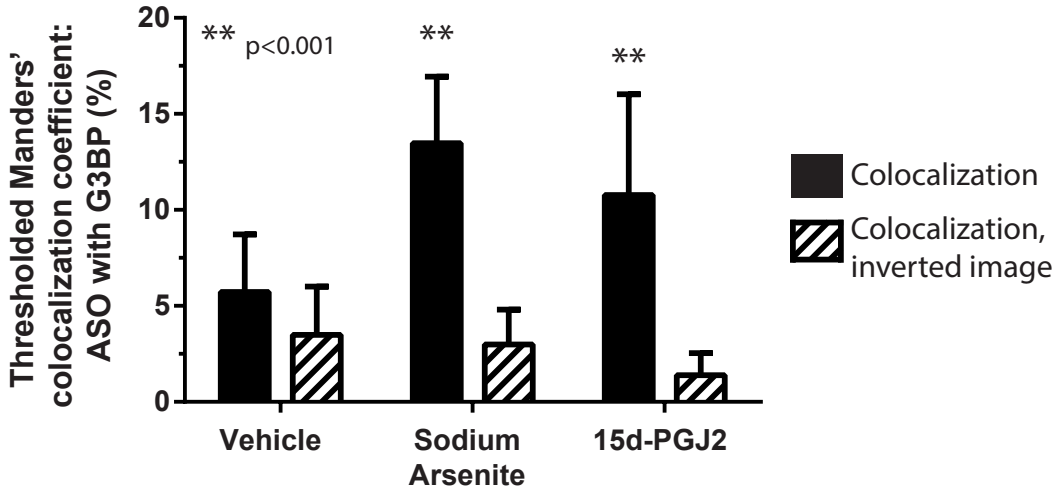

Supplementary Figure 13

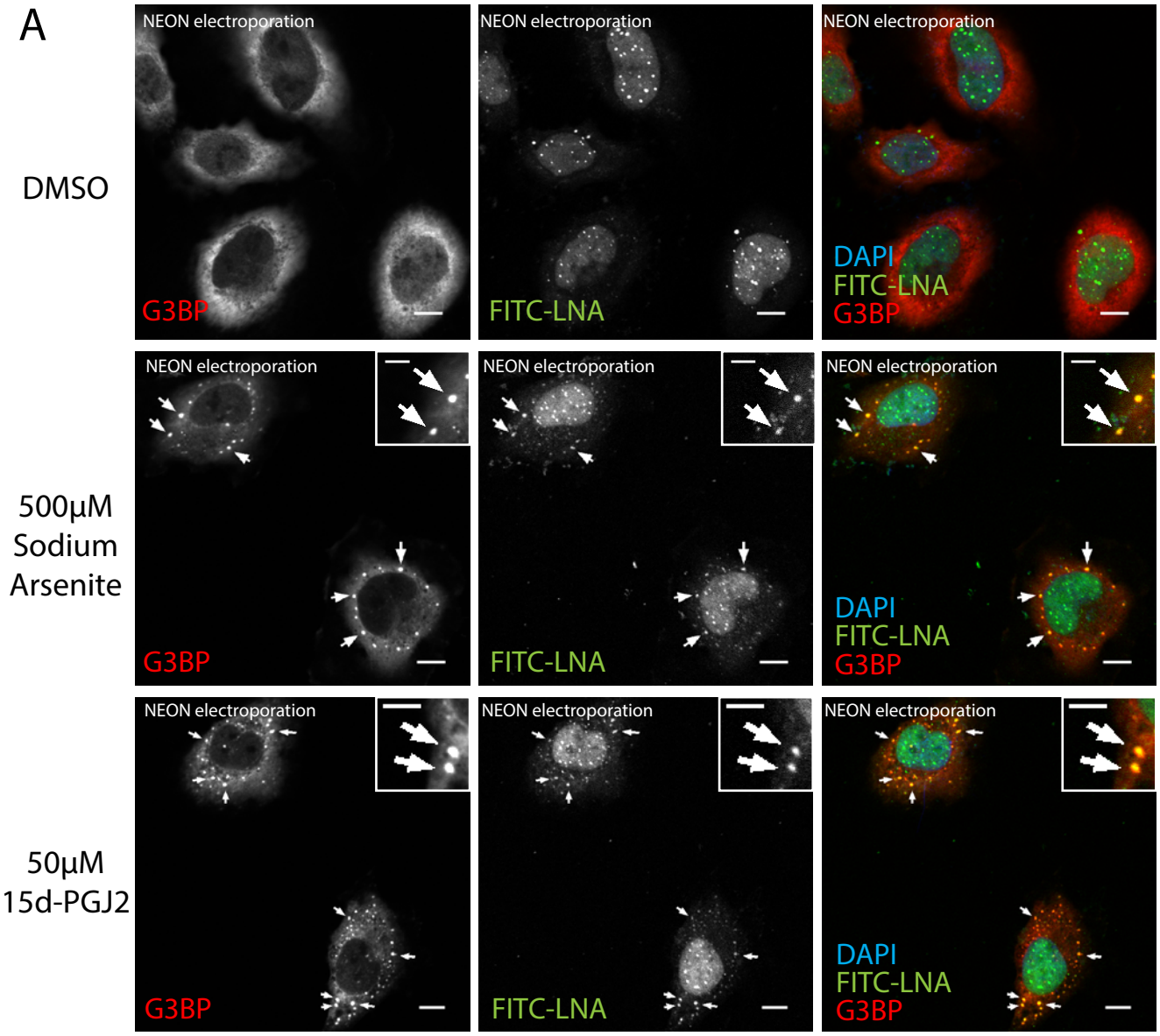

Supplementary Figure 14

A HA-FUS-WT

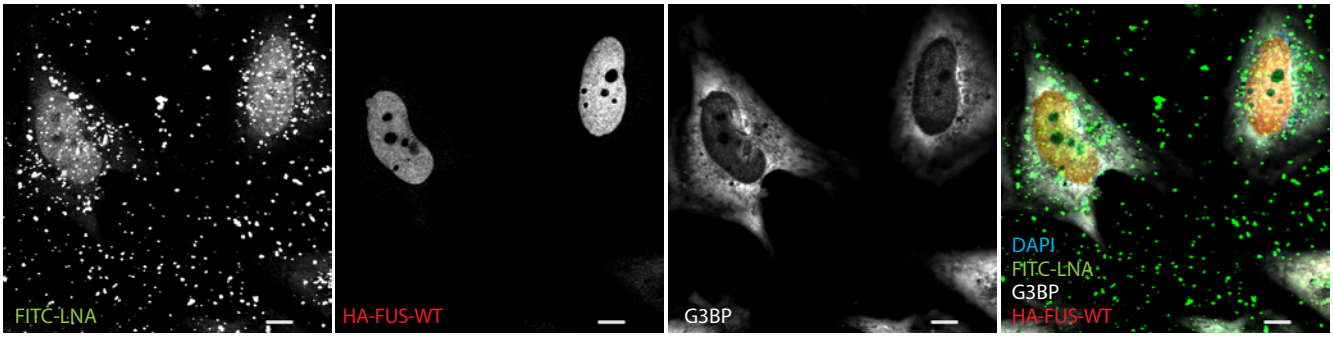

B HA-FUS-P525L

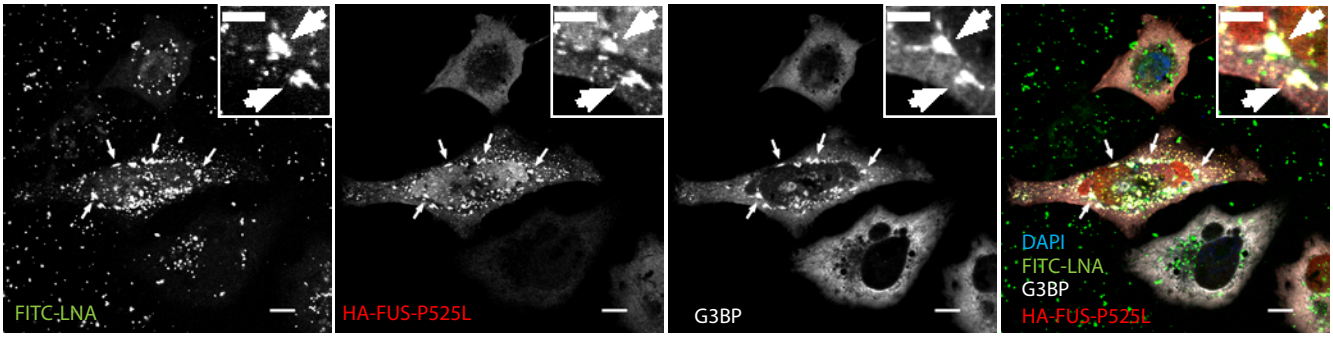

C

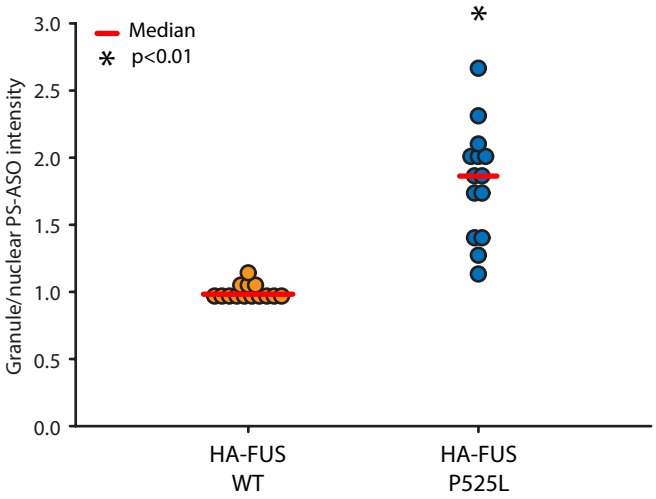

Supplementary Figure 15

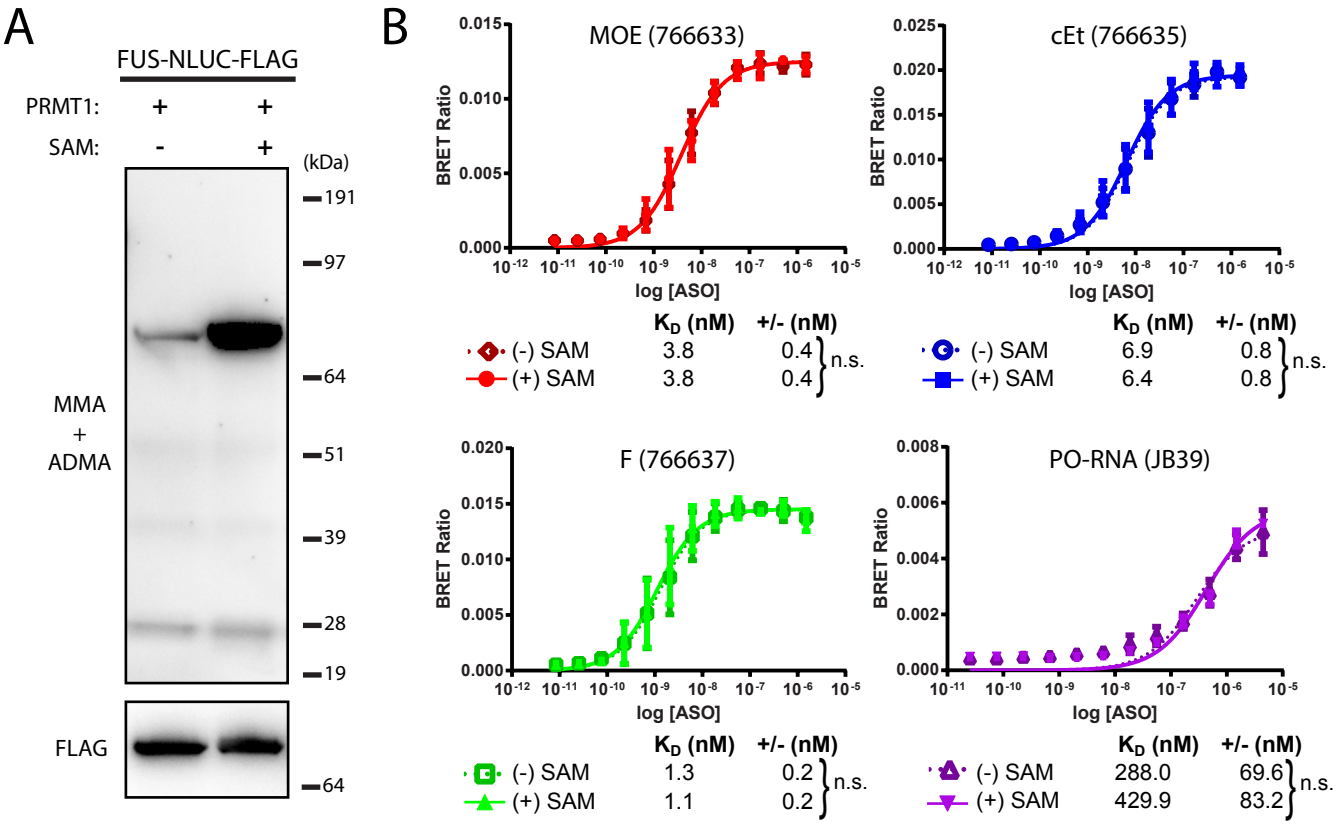

Supplementary Figure 16

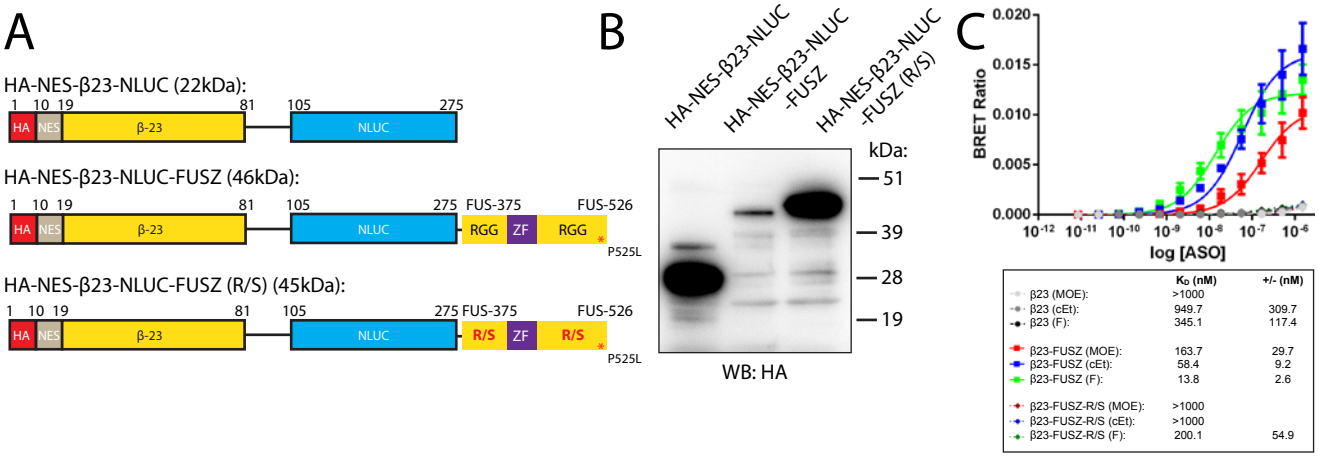

Supplementary Figure 17

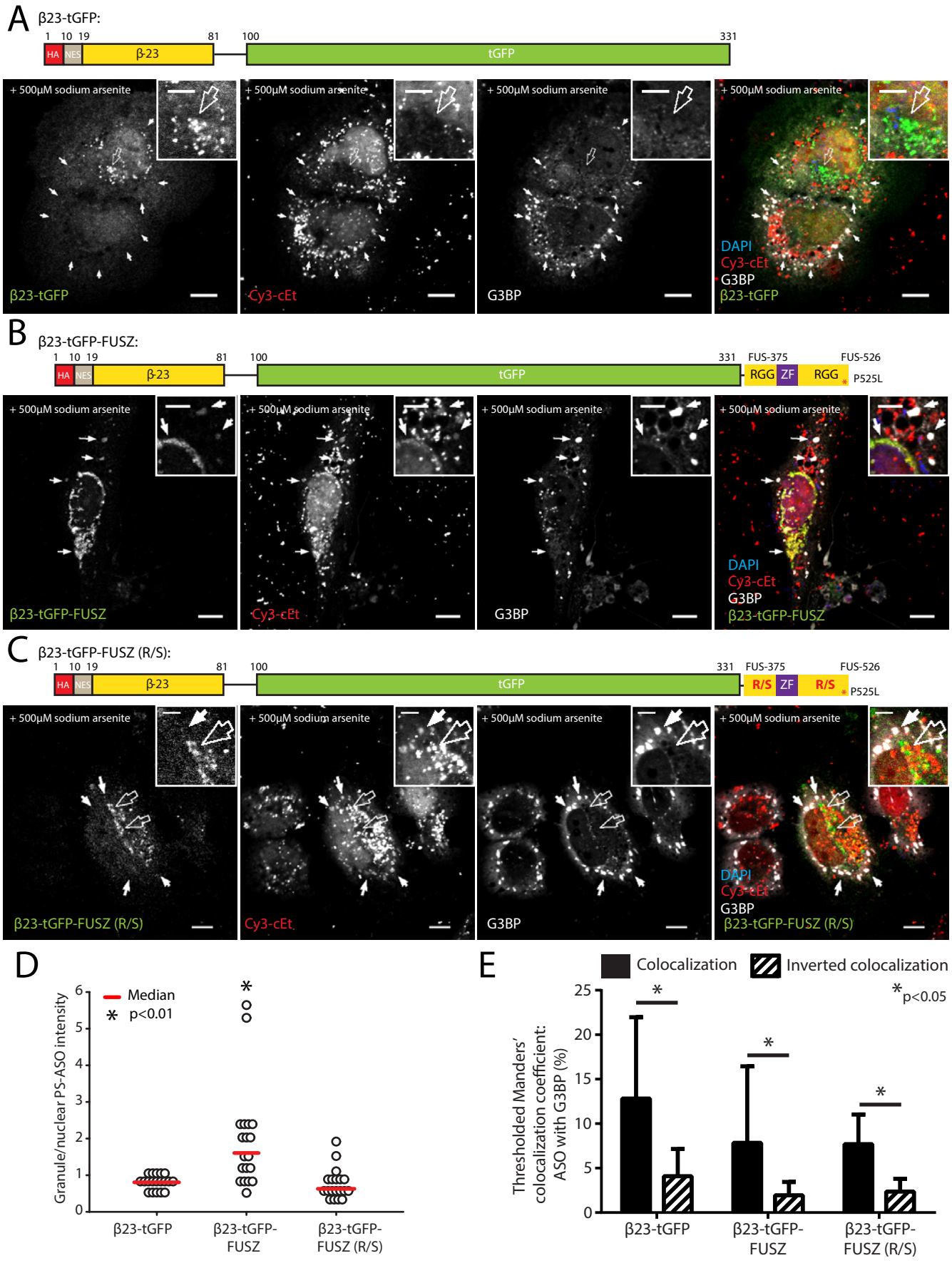

Supplementary Figure 18

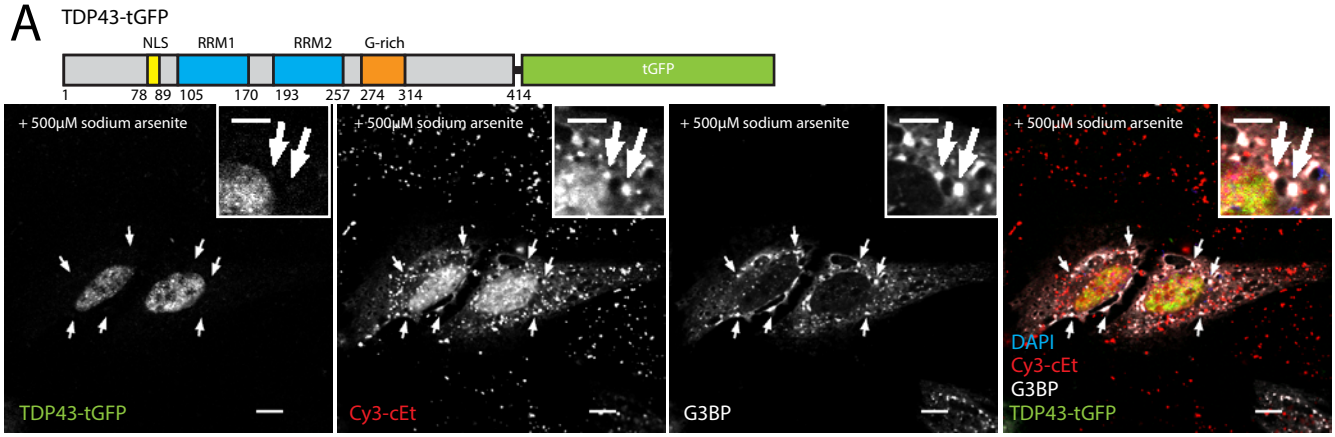

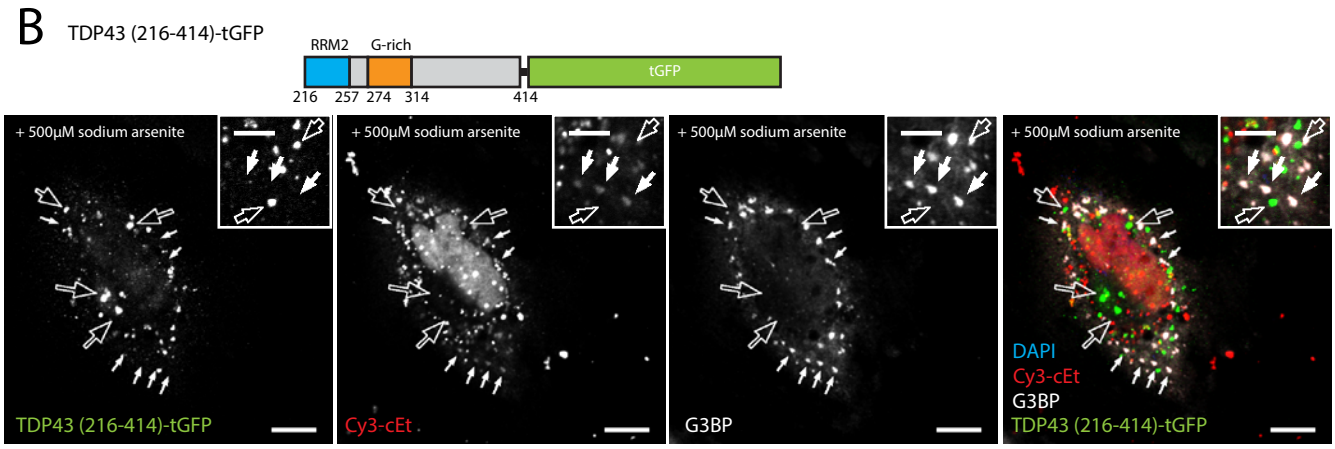

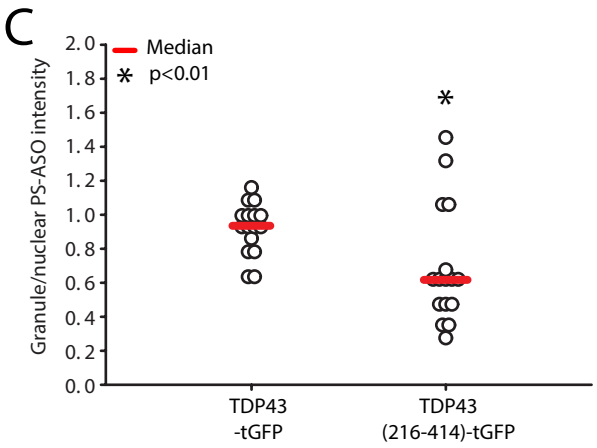

SUPPLEMENTARY FIGURE LEGENDS

Supplementary Figure 1. Cy3-labeled cEt PS-ASO delivered by electroporation is recruited to endogenous stress granules. (A) Representative confocal immunofluorescence images of HeLa cells electroporated with a Cy3-labeled cEt PS-ASO (ION-950432) under control conditions (DMSO) and after incubation of cells with eIF2α-dependent (sodium arsenite) or eIF2α-independent (15d-PGJ2) stress granule inducers for 1 h. Scale bars, 10μm. Insert scale bars, 5μm. (B) Colocalization between the Cy3-labeled cEt PS-ASO and G3BP was quantified by the thresholded Manders' colocalization coefficient method(** indicates $p<0.001$ vs. all other groups). Statistical analysis was performed using a univariate ANOVA with Tukey's HSD post hoc test (n=15 image fields per group), and error bars represent ± S.D.

Supplementary Figure 2. cEt PS-ASO is recruited to cytoplasmic G3BP-positive granules in A431 cells stably expressing tGFP-FUS-P525L. Representative confocal immunofluorescence images of A431 cells stably transduced with lentiviral particles (MOI ~5) containing tGFP alone, tGFP-FUS-WT, or tGFP-FUS-P525L. Scale bars, 10μm.

Supplementary Figure 3. Expression of HA-tagged FUS-P525L stimulates the recruitment of cEt PS-ASO to G3BP positive cytoplasmic granules. (A-B) Representative confocal immunofluorescence images of HeLa cells expressing HA-FUS-WT or HA-FUS-P525L. Cy3-labeled cEt PS-ASO (ION-598987) was transfected at 50 nM for 5 h. (C) ROI-based image quantification. Each data point represents one cell (n=15 cells per group), and statistical analysis was performed using the Kruskal-Wallis one-way analysis of variance (* indicates $p<0.01$). (D) Western blot analysis confirmed the expression of the recombinant proteins. Endogenous FUS levels were not substantially affected by expression of either HA-tagged FUS construct. GAPDH is included as a loading control. Approximate molecular masses are noted at the right in kDa.

Supplementary Figure 4. Cytoplasmic aggregation of poly(A) RNA is not the result of plasmid or cEt PS-ASO transfection. (A) Representative confocal immunofluorescence images of poly(A) RNA in untreated cells (UTC) or cells expressing tGFP. (B) Representative confocal

immunofluorescence images of poly(A) RNA in HeLa cells expressing tGFP. Cells were transfected with Cy3 labeled cEt PS-ASO (50nM for 5hrs, ION-598987). Scale bars, 10μm.

Supplementary Figure 5. Cytoplasmic tGFP-FUS-P525L granules do not recruit the *NEAT1* lncRNA. Representative confocal immunofluorescence images of *NEAT1* lncRNA in HeLa cells transiently expressing tGFP-FUS-WT or tGFP-FUS-P525L. Scale bars, 10μm.

Supplementary Figure 6. Expression of the tGFP-FUS and tGFP-PSF constructs does not substantially affect the levels of endogenous FUS or PSF, respectively. (A-B) Western blot analysis confirmed the expression of the recombinant proteins and endogenous (A) FUS or (B) PSF. GAPDH is included as a loading control. Approximate molecular masses are noted at the right in kDa.

Supplementary Figure 7. Cytoplasmic aggregates seeded by the TDP-43 C-terminal fragment do not recruit cEt PS-ASO. (A-C) Representative confocal immunofluorescence images of transfected A594-labeled cEt PS-ASO (50 nM for 5 h, ION-766635, arrows) in HeLa cells expressing (A) TDP43-tGFP, (B) TDP43-ΔNLS-tGFP, or (C) TDP43(216-414)-tGFP. Scale bars, 10μm. Insert scale bars, 5μm. (D) ROI-based image quantification. Each data point represents one cell (n=16 cells per group), and statistical analysis was performed using the Kruskal-Wallis one-way analysis of variance (* indicates $p<0.01$). (E) Western blot analysis confirmed the expression of the recombinant proteins. GAPDH is included as a loading control. Approximate molecular masses are noted at the right in kDa.

Supplementary Figure 8. Granule/nuclear localization of A647-MOE PS-ASO is not significantly affected by equimolar co-transfection with various Cy3 PS-ASOs (50nM each). This indicates that A647-MOE PS-ASO is a reliable signal intensity benchmark for Cy3-ASO normalization. Each data point represents one cell, and statistical analysis was performed using the Kruskal-Wallis one-way analysis of variance ($\alpha<0.05$).

Supplementary Figure 9. Subcellular distribution of transfected PS-ASOs in cells expressing tGFP. Representative confocal immunofluorescence images of transfected Cy3-

labeled ASOs of different 2' modifications (50 nM for 5 h, IONIS IDs are listed in the row headings) in HeLa cells expressing tGFP. Scale bars, 10μm.

Supplementary Figure 10. Subcellular distribution of transfected PS-ASOs in cells expressing tGFP-FUS-WT. Representative confocal immunofluorescence images of transfected Cy3-labeled ASOs of different 2' modifications (50 nM for 5 h, IONIS IDs are listed in the row headings) in HeLa cells expressing tGFP-FUS-WT. Scale bars, 10μm.

Supplementary Figure 11. Transfected PS-ASOs and G3BP localize to cytoplasmic tGFP-FUS-P525L granules. Representative confocal immunofluorescence images of transfected Cy3-labeled ASOs of different 2' modifications (50 nM for 5 h, IONIS IDs are listed in the row headings) in HeLa cells expressing tGFP-FUS-P525L. Scale bars, 10μm.

Supplementary Figure 12. FITC-labeled LNA PS-ASO localizes to stress granules formed by two different stress granule inducers. (A) Representative confocal immunofluorescence images of transfected FITC-labeled LNA PS-ASO (ION-391857, 50 nM for 5 h) in HeLa cells under control conditions (DMSO) and after incubation of cells with eIF2α-dependent (sodium arsenite) or eIF2α-independent (15d-PGJ2) stress granule inducers for 1. Scale bars, 10μm. Insert scale bars, 5μm. (B) Colocalization between the FITC-labeled LNA PS-ASO and G3BP was quantified by the thresholded Manders' colocalization coefficient method. (** indicates $p<0.001$ vs. all other groups). Statistical analysis was performed using a univariate ANOVA with Tukey's HSD post hoc test (n=15 image fields per group), and error bars represent ± S.D.

Supplementary Figure 13. FITC-labeled LNA PS-ASO delivered by electroporation is recruited to endogenous stress granules. (A) Representative confocal immunofluorescence images of HeLa cells electroporated with a FITC-labeled LNA PS-ASO (ION-391857) under control conditions (DMSO) and after incubation of cells with eIF2α-dependent (sodium arsenite) or eIF2α-independent (15d-PGJ2) stress granule inducers for 1 h. Scale bars, 10μm. Insert scale bars, 5μm. (B) Colocalization between the FITC-labeled LNA PS-ASO and G3BP was quantified by the thresholded Manders' colocalization coefficient method (** indicates $p<0.001$ vs.

all other groups). Statistical analysis was performed using a univariate ANOVA with Tukey's HSD post hoc test (n=15 image fields per group), and error bars represent ± S.D.

Supplementary Figure 14. Expression of HA-tagged FUS-P525L recruits LNA PS-ASO to G3BP positive cytoplasmic granules. (A, B) Representative confocal immunofluorescence images of HeLa cells transfected with a FITC-labeled LNA PS-ASO (ION-391857, 50 nM for 5 h) in cells expressing (A) HA-FUS-WT or (B) HA-FUS-P525L. (C) ROI-based image quantification. Each data point represents one cell (n=14 cells per group), and statistical analysis was performed using the Kruskal-Wallis one-way analysis of variance (* indicates $p<0.01$).

Supplementary Figure 15. PRMT1-mediated arginine methylation of FUS does not affect its PS-ASO binding properties. (A) FUS with C-terminal Nanoluciferase and FLAG tags was *in vitro* transcribed and translated, methylated by protein arginine methyltransefrase 1 (PRMT1) in the presence or absence of the essential methyl donor S-adenosyl methionine (SAM), and anti-FLAG affinity purified. Western blotting with a combination of anti-asymmetric dimethyl arginine and anti-mono methyl arginine antibodies confirmed the deposition of SAM-dependent arginine methylation on FUS-NLUC-FLAG. Approximate molecular masses are noted at the right in kDa. (B) NanoBRET binding assays with methylated (+SAM) and unmethylated (-SAM) FUS-NLUC-FLAG were performed for the following ASOs: MOE: ION-766633, cEt: ION-766635, F: ION-766637, PO-RNA: JB-39. Binding experiments were performed n=3 times per group and error bars represent ± S.D. Relative K_D values are presented as average ± S.D. Statistical analysis on the binding curve affinities (K_D) and amplitudes (Bmax) was performed using the univariate ANOVA with Tukey's HSD post hoc.

Supplementary Figure 16. The FUS-Z domain fused to the artificial β-sheet protein β23 is sufficient to bind PS-ASOs *in vitro.* (A) Schematic representation of three constructs: HA-NES-β23-NLUC, HA-NES-β23-NLUC-FUSZ, and HA-NES-β23-NLUC-FUSZ (R/S). (B) Western blot analysis confirmed the expression of the recombinant proteins. Approximate molecular masses are noted at the right in kDa. (C) NanoBRET binding assays for the β23-fusion proteins were performed with A594-labeled PS-ASOs (MOE: ION-766633, cEt: ION-766635, F: ION-

766637). Binding experiments were performed in triplicate and error bars represent ± S.D. Relative K_D values are presented as average ± S.D.

Supplementary Figure 17. Recruitment of cEt PS-ASO is a specific property of endogenous stress granules and cytoplasmic β23-FUS-Z granules. (A-C) Representative confocal immunofluorescence images of a transfected Cy3-labeled cEt PS-ASO (ION-598987, 50 nM for 5 h) in HeLa cells expressing (A) β23-tGFP, (B) β23-tGFP-FUSZ, or (C) β23-tGFP-FUSZ (R/S). Cells were treated with 500 µM sodium arsenite for 1 h. Scale bars, 10µm. Insert scale bars, 5µm. (D) The average granule/nuclear pixel intensity was measured using ROI-based image quantification. Each data point represents one cell (n=18-19 cells per group), and statistical analysis was performed using the Kruskal-Wallis one-way analysis of variance (* indicates $p<0.01$). (E) Colocalization between the cEt PS-ASO and G3BP was quantified by the thresholded Manders' colocalization coefficient method(* indicates $p<0.05$ vs. each corresponding inverted colocalization control). Statistical analysis was performed using a univariate ANOVA with Tukey's HSD post hoc test (n=18-19 cells per group), and error bars represent ± S.D.

Supplementary Figure 18. Endogenous stress granules but not TDP43 C-terminal aggregates recruit cEt PS-ASO within the same cell (A, B) Representative confocal immunofluorescence images of a transfected Cy3-labeled cEt PS-ASO (ION-598987, 50 nM for 5 h) in HeLa cells expressing (A) TDP43-tGFP or (B) TDP43 (216-414)-tGFP. Cells were treated with 500 µM sodium arsenite for 1 h. (C) The average granule/nuclear pixel intensity was measured using ROI-based image quantification. Each data point represents one cell (n=16 cells per group), and statistical analysis was performed using the Kruskal-Wallis one-way analysis of variance (* indicates $p<0.01$).

Supplementary Table 1: DNA plasmid constructs

Expression Plasmids and Cloning Information						
Name	**Template/ Source**	**Destination**	**5' Site**	**3' Site**	**Method**	**Tag**
pCMV6-AN-tGFP-FUS-WT	Origene (RG201808)	pCMV6-AN-tGFP (Origene, PS100019)	AsiSI	PmeI	PCR (JB1,JB2)	tGFP (N-terminal)
pCMV6-AN-tGFP-FUS-P525L	Origene (RG201808), Site-directed mutagenesis (JB3,JB4)	pCMV6-AN-tGFP (Origene, PS100019)	AsiSI	PmeI	PCR (JB1,JB5)	tGFP (N-terminal)
pCMV6-HA-FUS-WT	Annealed insert (JB43, JB44)	pCMV6-AN-tGFP-FUS-WT	BamHI	AsiSI	Subcloning	HA (N-terminal)
pCMV6-HA-FUS-P525L	Annealed insert (JB43, JB44)	pCMV6-AN-tGFP-FUS-P525L	BamHI	AsiSI	Subcloning	HA (N-terminal)
EGFP-PSF-WT	Genscript (OHu23607C)	pcDNA3.1-N-EGFP	KpnI	XhoI	Purchased	EGFP (N-terminal)
EGFP-PSF-ΔNLS	Genscript (OHu23607M)	pcDNA3.1-N-EGFP	KpnI	XhoI	Purchased	EGFP (N-terminal)
NLUC-HA	NEB-IVT-YBX1-NLUC-HA (unpublished)	NEB-IVT	NdeI	BlpI	PCR (JB6,JB7)	HA (C-terminal)
NEB-NLUC	pFN31K-NLUC-P54nrb (Vickers and Crooke, 2016)	NEB-IVT	NdeI	XhoI	PCR (JB8,JB9)	None
NEB-NLUC-FUS-HA (N-term NLUC)	pCMV6-AN-tGFP-FUS-P525L	NEB-NLUC	XhoI	BlpI	PCR (JB10,JB11)	HA (C-terminal)
NEB-FUS-NLUC-HA (C-term NLUC)	pCMV6-AN-tGFP-FUS-P525L	NEB-IVT-YBX1-NLUC-HA (unpublished)	NdeI	XhoI	PCR (JB12,JB13)	HA (C-terminal)
NEB-FUS-N-NLUC-HA	pCMV6-AN-tGFP-FUS-P525L	NEB-IVT-YBX1-NLUC-HA (unpublished)	NdeI	XhoI	PCR (JB12,JB14)	HA (C-terminal)
NEB-FUS-NR-NLUC-HA	pCMV6-AN-tGFP-FUS-P525L	NEB-IVT-YBX1-NLUC-HA	NdeI	XhoI	PCR (JB12,JB15)	HA (C-terminal)

		(unpublished)				
NEB-FUS-RRM-NLUC-HA	pCMV6-AN-tGFP-FUS-P525L	NEB-IVT-YBX1-NLUC-HA (unpublished)	NdeI	XhoI	PCR (JB15,JB16)	HA (C-terminal)
NEB-FUS-Z-NLUC-HA	pCMV6-AN-tGFP-FUS-P525L	NEB-IVT-YBX1-NLUC-HA (unpublished)	NdeI	XhoI	PCR (JB13,JB17)	HA (C-terminal)
NEB-FUS-NLUC-FLAG	I1: pCMV6-AN-tGFP-FUS-P525L I2: pFN31K-NLUC-P54nrb (Vickers and Crooke, 2016)	NEB-IVT	I1: NdeI I2: NotI	I1: NotI I2: BlpI	I1: PCR (JB12,JB18) I2: PCR (JB19,JB20)	FLAG (C-terminal)
NEB-FUS-ΔZF-NLUC-FLAG	I1: NEB-FUS-NLUC-FLAG I2: NEB-FUS-NLUC-FLAG	NEB-FUS-NLUC-FLAG	I1: NdeI I2: PmeI (blunt)	I1: (blunt) I2: NotI	I1: PCR (JB12,JB21) I2: PCR (JB22,JB23)	FLAG (C-terminal)
NEB-FUS-R/S-NLUC-FLAG	FUS-R/S gBlock (IDT)	NEB-FUS-ΔZF-NLUC-FLAG	EcoRI	NotI	PCR (JB24,JB25)	FLAG (C-terminal)
pLVX-tGFP	pCMV6-AN-tGFP (Origene, PS100019)	pLVX-IRES-Puro (Clontech, 632183)	V: XhoI/Klenow I: BamHI/Klenow	NotI	Subcloning	None
pLVX-tGFP-FUS-WT	pCMV6-AN-tGFP-FUS-WT	pLVX-IRES-Puro (Clontech, 632183)	V: XhoI/Klenow I: BamHI/Klenow	NotI	Subcloning	tGFP (N-terminal)
pLVX-tGFP-FUS-P525L	pCMV6-AN-tGFP-FUS-P525L	pLVX-IRES-Puro (Clontech, 632183)	V: XhoI/Klenow I: BamHI/Klenow	NotI	Subcloning	tGFP (N-terminal)
pCMV6-AC-HA-NES-β23-tGFP	HA-NES-β23 gBlock (IDT)	pCMV6-AC-tGFP (Origene, PS100010)	BamHI	XhoI	PCR (JB26,JB27)	(Multiple)
HA-NES-β23-tGFP-FUS-Z (WT)	pCMV6-AN-tGFP-FUS-Z (WT) (unpublished)	pCMV6-AC-HA-NES-β23-tGFP	PspOMI	PmeI	Subcloning	(Multiple)
HA-NES-β23-tGFP-FUS-Z (R/S)	pCMV6-AN-tGFP-FUS-Z (R/S) (unpublished)	pCMV6-AC-HA-NES-β23-tGFP	PspOMI	PmeI	Subcloning	(Multiple)

NEB-HA-NES-β23-NLUC	HA-NES-β23 gBlock (IDT)	NEB-FUS-NLUC-FLAG	NdeI	NotI	PCR (JB28,JB29)	HA (N-terminal)
NEB-HA-NES-β23-NLUC-FUS-Z (WT)	NEB-HA-NLUC-FUS-Z (WT) (unpublished)	NEB-HA-NES-β23-NLUC	XapI	HindIII	Subcloning	HA (N-terminal)
NEB-HA-NES-β23-NLUC-FUS-Z (R/S)	NEB-HA-NLUC-FUS-Z (R/S) (unpublished)	NEB-HA-NES-β23-NLUC	XapI	HindIII	Subcloning	HA (N-terminal)
NEB-FUSZ-NT-RGG-NLUC-HA	pCMV6-AN-tGFP-FUS-P525L	NEB-IVT-YBX1-NLUC-HA (unpublished)	NdeI	XhoI	PCR (JB17,JB30)	HA (C-terminal)
NEB-FUSZ-CT-RGG-NLUC-HA	pCMV6-AN-tGFP-FUS-P525L	NEB-IVT-YBX1-NLUC-HA (unpublished)	NdeI	XhoI	PCR (JB13,JB31)	HA (C-terminal)
NEB-FUSZ-NT (R/S)-NLUC-HA	FUSZ-NT(R/S) gBlock	NEB-IVT-YBX1-NLUC-HA (unpublished)	NdeI	XhoI	PCR (JB32,JB33)	HA (C-terminal)
NEB-FUSZ-CT (R/S)-NLUC-HA	FUSZ-CT(R/S) gBlock	NEB-IVT-YBX1-NLUC-HA (unpublished)	NdeI	XhoI	PCR (JB34,JB35)	HA (C-terminal)
NEB-FUS-R1-NLUC-HA	pCMV6-AN-tGFP-FUS-WT	NEB-IVT-YBX1-NLUC-HA (unpublished)	NdeI	XhoI	PCR (JB45, JB15)	HA (C-terminal)
NEB-FUS-R2-NLUC-HA	pCMV6-AN-tGFP-FUS-WT	NEB-IVT-YBX1-NLUC-HA (unpublished)	NdeI	XhoI	PCR (JB46, JB15)	HA (C-terminal)
pCMV6-AC-TDP43-tGFP	Origene (RG210639)	-	SgfI	MluI	Purchased	tGFP (C-terminal)
pCMV6-AC-TDP43 (ΔNLS)-tGFP	Origene (RG210639)	pCMV6-AC-tGFP	BamHI	NotI	PCR (JB36,JB37)	tGFP (C-terminal)
pCMV6-AC-TDP43 (216-414)-tGFP	Origene (RG210639)	pCMV6-AC-tGFP	BamHI	NotI	PCR (JB37,JB38)	tGFP (C-terminal)

Supplementary Table 2: Cloning primers

Primers		
Name	**Sequence**	**Construct**

JB1	5’-CATCATGCGATCGCCATGGCCTCAAACG-3’	tGFP-FUS-WT
JB2	5’-CATCATGCGGCCGCTTAATACGGCCTCTCCCTGCGATC-3’	tGFP-FUS-WT
JB3	5’-GATCGCAGGGAGAGGCTGTATACGCGTACGCGG-3’	tGFP-FUS-P525L
JB4	5’-CCGCGTACGCGTATACAGCCTCTCCCTGCGATC-3’	tGFP-FUS-P525L
JB5	5’-CATCATGCGGCCGCTTAATACAGCCTCTCCCTGCGATC-3’	tGFP-FUS-P525L
JB6	5’-CATCATCATATGGTCTTCACACTCGAAGATTTCGTTGG-3’	NLUC-HA
JB7	5’-CATCATGCTCAGCTTAAGCGTAATCTGGAACATCGTATGGGTAC-3’	NLUC-HA
JB8	5’-CATCATCATATGGTCTTCACACTCGAAGATTTCGTTGGG-3’	NEB-NLUC
JB9	5’-CTGCATGGCGATCGCGGCG-3’	NEB-NLUC
JB10	5’-CATCATCTCGAGCATGGCCTCAAACGATTATAC-3’	NEB-NLUC-FUS-HA
JB11	5’-CATCATGCTCAGCTTAAGCGTAATCTGGAACATCGTATGGGTAATACAGCCTCTCCCTGCGATCCTGTC-3’	NEB-NLUC-FUS-HA
JB12	5’-CATCATCATATGGCCTCAAACGATTATACCCAACAAGC-3’	(Multiple)
JB13	5’-CATCATCTCGAGATACAGCCTCTCCCTGCGATCC-3’	(Multiple)
JB14	5’-CATCATCTCGAGGTCTGAATTATCCTGTTCGGAGTCATGACGTG-3’	NEB-FUS-N-NLUC-HA
JB15	5’-CATCATCTCGAGAAAGTCTGCCCGGCGAGTAG-3’	(Multiple)
JB16	5’-CATCATCATATGAGCAACAACACCATCTTTGTGCAAGG-3’	NEB-FUS-RRM-NLUC-HA
JB17	5’-CATCATCATATGAGCAATCGGGGTGGTGGCAATG-3’	(Multiple)
JB18	5’-TCTCGAGCGGCCGCGTAC-3’	NEB-FUS-NLUC-FLAG
JB19	5’-CATCATGCGGCCGCTGATGGTCTTCACACTCGAAGATTTCGTTGGG-3’	NEB-FUS-NLUC-FLAG
JB20	5’-CATCATGCTCAGCTTACTTATCGTCGTCATCCTTGTAATCCGCCAGAATGCGTTCGCACAG-3’	NEB-FUS-NLUC-FLAG

JB21	5’-TCGCTGCTGTCCTCCACCGCCAC-3’	NEB-FUS-ΔZF-NLUC-FLAG
JB22	5’-CATCATGTTTAAACACCCAGGAGGGGGACCAGGTG-3’	NEB-FUS-ΔZF-NLUC-FLAG
JB23	5’-CATCATGCGGCCGCGTACGCGTATAC-3’	NEB-FUS-ΔZF-NLUC-FLAG
JB24	5’-GGTAAAGAATTCTCCGGAAATCCGATAAAGGTG-3’	NEB-FUS-R/S-NLUC-FLAG
JB25	5’-GCATCAGCGGCCGCGTAC-3’	NEB-FUS-R/S-NLUC-FLAG
JB26	5’-CATCATGGATCCGCCACCATGGACC-3’	(Multiple)
JB27	5’-ATGATGCTCGAGGGCGGCG-3’	(Multiple)
JB28	5’-CATCATCATATGGCCACCATGGACCAGTACCCATACG-3’	NEB-HA-NES-β23-NLUC
JB29	5’-CATCATGCGGCCGCAGATGCTCGAGGGCGGCG-3’	NEB-HA-NES-β23-NLUC
JB30	5’-CATCATCTCGAGCTGCTGTCCTCCACCGCCA-3’	NEB-FUSZ-NT-RGG-NLUC-HA
JB31	5’-ATCCATCATATGCCAGGAGGGGGACCAGGTG-3’	NEB-FUSZ-CT-RGG-NLUC-HA
JB32	5’-ACTCATCATATGAACTCCGGCGGCGGTAATG-3’	NEB-FUSZ-NT (R/S)-NLUC-HA
JB33	5’-CATCATCTCGAGGTATAAACGCTCGCGACGATCCTG-3’	NEB-FUSZ-NT (R/S)-NLUC-HA
JB34	5’-ACTCATCATATGAACCGTGGCGGAGGTAACG-3’	NEB-FUSZ-CT (R/S)-NLUC-HA
JB35	5’-CATCATCTCGAGATAAAGGGACTCGGAACTATCCTGGGAATG-3’	NEB-FUSZ-CT (R/S)-NLUC-HA
JB36	5’-CATCATGGATCCGCCACCATGGATGCTTCATCAGCAGTGAAAGTGAAAAGAGC-3’	pCMV6-AC-TDP43 (ΔNLS)-tGFP
JB37	5’-CATCATGCGGCCGCGTACGCGTCATTC-3’	(Multiple)
JB38	5’-CATCATGGATCCGCCACCATGGATGTGATGGATGTCTTCATCCCCAAGCCATTC-3’	pCMV6-AC-TDP43 (216-414)-tGFP
JB43	5’-GATCGCCACCATGTACCCATACGATGTTCCAGATTACGCTAT-3’	(Multiple)

JB44	5’-AGCGTAATCTGGAACATCGTATGGGTACATGGTGGC-3’	(Multiple)
JB45	5’-CATCATCATATGCGTGGAGGCCGCGGC-3’	NEB-FUS-R1-NLUC-HA
JB46	5’- CATCATCATATGAGAGGTCGTGGAGGTGGCC	NEB-FUS-R2-NLUC-HA

Supplementary Table 3: gBlock synthetic DNA constructs

gBlocks (Integrated DNA Technologies)		
Name	**Nucleotide**	**Protein**
FUS-R/S gBlock	5’- GGTAAAGAATTCTCCGGAAATCCGATA AAGGTGTCTTTCGCTACTAGACGGGCT GATTTCAACAGCGGTGGCGGTAACGG GAGTGGCGGGTCCGGTAGTGGTGGCC CGATGGGTTCTGGGGGTTATGGTGGC GGTGGGTCAGGTGGCGGTGGTAGTGG GGGCTTTCCGAGTGGTGGCGGCGGAG GTGGTGGACAGCAGCGGGCGGGAGAT TGGAAATGCCCTAACCCAACGTGTGAA AACATGAACTTCTCATGGAGAAATGAGT GTAACCAATGCAAAGCCCCCAAACCGG ACGGGCCGGGTGGTGGCCCGGGTGGT AGCCATATGGGCGGCAACTATGGCGAT GATTCAAGTGGTGGAAGTGGCGGTTAT GATTCTGGTGGTTATAGTGGATCTGGT GGTGATAGCGGTGGATTTAGCGGCGG AAGTGGTGGAGGCGATAGCGGGGGTT TTGGCCCGGGCAAAATGGATAGCAGC GGCGAACATAGCCAGGATAGCAGCGA AAGCCTGTATACGCGTACGCGGCCGCT GATGC-3’	*NT*_GKEFSGNPIKVSFATRRADF**NSGGGN GSGGSGSGGPMGSGGYGGGGSGGGGS GGFPSGGGGGGGQQ<u>RAGDWKCPNPTC ENMNFSWRNECNQCKAPKPDG</u>PGGGP GGSHMGGNYGDDSSGGSGGYDSGGYS GSGGDSGGFSGGSGGGDSGGFGPGKM DSSGEHSQDSSESLY**TRTRPLM_*CT* -Bold indicates FUS-Z domain (with R/S mutations) -Underline indicates ZF region
2XNLS-HA-β23 gBlock	5’- CATCATGGATCCGCCACCATGGACCCC AAGAAGAAGAGGAAGGTGGACCCCAA GAAGAAGAGGAAGGTGTACCCATACGA TGTTCCAGATTACGCTATGGATTATAAC ATCCAGTTCCACAATAATGGTAATGAGA TCCAGTTCGAGATCGACGATTCTGGTG GTGATATTGAAATTGAGATCCGCGGCC	*NT*- <u>MDPKKKRKVDPKKKRKVYPYDVPDYA</u>**MD YNIQFHNNGNEIQFEIDDSGGDIEIEIRGPG GRVHIQLNDGHGHIKVDFHNDGGELQIDM H**TSGSAASAAGAGEAAA-*CT* -Bold indicates β23 -Underline indicates 2XNLS-HA

	CGGGTGGCCGTGTCCACATCCAGCTCA ACGATGGTCATGGTCACATCAAGGTCG ACTTCCACAACGACGGCGGCGAACTTC AAATTGATATGCACACCAGCGGCAGCG CCGCCAGCGCCGCCGGCGCCGGCGA GGCCGCCGCCCTCGAGCATCAT-3’	
HA-NES-β23 gBlock	5’- CATCATGGATCCGCCACCATGGACCAG TACCCATACGATGTTCCAGATTACGCTC TGGAGCTGCTGGAGGACCTGACCCTG ATGGATTATAACATCCAGTTCCACAATA ATGGTAATGAGATCCAGTTCGAGATCG ACGATTCTGGTGGTGATATTGAAATTGA GATCCGCGGCCCGGGTGGCCGTGTCC ACATCCAGCTCAACGATGGTCATGGTC ACATCAAGGTCGACTTCCACAACGACG GCGGCGAACTTCAAATTGATATGCACA CCAGCGGCAGCGCCGCCAGCGCCGCC GGCGCCGGCGAGGCCGCCGCCCTCGA GCATCAT-3’	*NT*- MDQYPYDVPDYALELLEDLTL**MDYNIQFH NNGNEIQFEIDDSGGDIEIEIRGPGGRVHI QLNDGHGHIKVDFHNDGGELQIDMH**TSG SAASAAGAGEAAA-*CT* -Bold indicates β23 -Underline indicates HA-NES
FUSZ-NT(R/S) gBlock	5’- AACTCCGGCGGCGGTAATGGAAGTGG CGGCAGCGGGTCGGGCGGCCCAATGG GTAGCGGCGGTTACGGGGGAGGTGGC TCTGGGGGAGGCGGAAGTGGAGGATT CCCGTCCGGCGGGGGGGGTGGAGGC GGCCAACAGCGTGCGGGCGATTGGAA GTGTCCCAACCCAACATGTGAGAACAT GAATTTCTCCTGGCGTAACGAGTGCAA CCAATGTAAGGCGCCAAAGCCAGACG GGCCGGGTGGTGGGCCTGGGGGGAG CCACATGGGCGGCAACTATGGAGACG ACCGTCGCGGAGGCCGCGGGGGGTAC GACCGTGGGGGTTATCGTGGCCGCGG GGGAGACCGTGGGGGTTTCCGTGGTG GACGTGGTGGCGGTGATCGCGGCGGC TTTGGTCCGGGAAAAATGGACTCCCGT GGCGAGCACCGCCAGGATCGTCGCGA GCGTTTATAC-3’	*NT*- NSGGGNGSGGSGSGGPMGSGGYGGGG SGGGGSGGFPSGGGGGGGQQ<u>RAGDWK CPNPTCENMNFSWRNECNQCKAPKPDG</u> PGGGPGGSHMGGNYGDDRRGGRGGYD RGGYRGRGGDRGGFRGGRGGGDRGGF GPGKMDSRGEHRQDRRERLY-*CT* -Underline indicates ZF region
FUSZ-CT(R/S) gBlock	5’- AACCGTGGCGGAGGTAACGGACGCGG AGGGCGTGGACGTGGAGGGCCTATGG GACGTGGGGGGTACGGAGGCGGCGG ATCGGGAGGAGGAGGCCGCGGAGGAT TCCCAAGCGGTGGAGGGGGCGGGGGT GGACAACAGCGCGCAGGCGACTGGAA GTGCCCTAATCCTACATGTGAAAATATG AACTTCAGCTGGCGCAACGAATGTAAC CAGTGCAAAGCTCCCAAACCAGACGGA CCGGGCGGAGGTCCGGGTGGATCCCA CATGGGCGGAAACTACGGAGATGACTC AAGCGGCGGCTCCGGCGGATACGATA GTGGAGGATATAGTGGGTCCGGCGGC GACAGCGGAGGTTTCTCCGGTGGATCA GGGGGAGGCGACTCGGGGGGCTTCG GACCCGGTAAAATGGATAGTTCTGGGG	*NT*- NRGGGNGRGGRGRGGPMGRGGYGGG GSGGGGRGGFPSGGGGGGGQQ<u>RAGDW KCPNPTCENMNFSWRNECNQCKAPKPD G</u>PGGGPGGSHMGGNYGDDSSGGSGGY DSGGYSGSGGDSGGFSGGSGGGDSGGF GPGKMDSSGEHSQDSSESLY-*CT* -Underline indicates ZF region

	AACATTCCCAGGATAGTTCCGAGTCCC TTTAT-3’	

Supplementary Table 4: ASOs

In the table below, deoxyribonucleotides are in plain font, ribonucleotides are underlined, 2’-modified nucleotides are in bold font, and phosphorothioate (PS) linkages are indicated with asterisks (*).

ASOs			
IONIS ID	**Sequence**	**RNA Target**	**2’ Modification**
446654	5’-Cy3-**C*T*G*C*T***A*G*C*C*T*C*T*G*G*A***T*T*T*G*A**-3’	PTEN	MOE
598987	5’-Cy3-**C*T*G*C*T***A*G*C*C*T*C*T*G*G*A***T*T*T*G*A**-3’	PTEN	cEt
391857	5’-FITC-**C*T*G*C*T***A*G*C*C*T*C*T*G*G*A***T*T*T*G*A**-3’	PTEN	LNA
626825	5’-Cy3-**C*T*G*C*T***A*G*C*C*T*C*T*G*G*A***T*T*T*G*A**-3’	PTEN	α-fluoro
851810	5’-AF647-**C*T*G*C*T***A*G*C*C*T*C*T*G*G*A***T*T*T*G*A**-3’	PTEN	MOE
766633	5’-AF594-**C*T*G*C*T***A*G*C*C*T*C*T*G*G*A***T*T*T*G*A**-3’	PTEN	MOE
766635	5’-AF594-**C*T*G*C*T***A*G*C*C*T*C*T*G*G*A***T*T*T*G*A**-3’	PTEN	cEt
766637	5’-AF594-**C*T*G*C*T***A*G*C*C*T*C*T*G*G*A***T*T*T*G*A**-3’	PTEN	α-fluoro
950431	5’-Cy3-**C*C*T*T*C***C*C*T*G*A*A*G*G*T*T***C*C*T*C*C**-3’	None	cEt
950432	5’-Cy3-**T*A*G*T*G***C*G*G*A*C*C*T*A*C*C***C*A*C*G*A**-3’	None	cEt
XL198	5’-Cy3-C*T*G*C*T*A*G*C*C*T*C*T*G*G*A*T*T*T*G*A-3’	PTEN	DNA
JB39	5’-AF594-<u>CUGCUAGCCUCUGGAUUUGA</u>-3’	PTEN	RNA
JB40	5’-CTGCTAGCCTCTGGATTTGA-3’	PTEN	DNA
JB41	5’-C*T*G*C*T*A*G*C*C*T*C*T*G*G*A*T*T*T*G*A-3’	PTEN	DNA
JB42	5’-<u>C*U*G*C*U*A*G*C*C*U*C*U*G*G*A*U*U*U*G*A</u>-3’	PTEN	RNA